Article:
Wei, M., Qian, F., Du, W. et al. (2018) Study on the integration of fluid catalytic cracking unit in refinery with solvent-based carbon capture through process simulation. Fuel, 219. pp. 364-374. ISSN: 0016-2361

https://doi.org/10.1016/j.fuel.2018.01.066

Study on the integration of Fluid Catalytic Cracking Unit in Refinery with Solvent-based Carbon Capture through Process Simulation

Min Wei[a], Feng Qian[a,*], Wenli Du[a], Jun Hu[b], Meihong Wang[c,*], Xiaobo Luo[c], Minglei Yang[a]

[a]. *Key Laboratory of Advanced Control and Optimization for Chemical Processes, Ministry of Education, School of Information Science and Engineering, East China University of Science and Technology, Shanghai 200237, China*

[b]. School of Chemistry and Molecular Engineering, *East China University of Science and Technology, Shanghai 200237, China*

[c]. *Department of Chemical and Biological Engineering, The University of Sheffield, Sheffield, Sheffield S1 3JD, United Kingdom*

*. Corresponding Author：

E-mail address: meihong.wang@sheffield.ac.uk (M. Wang),

fqian@ecust.edu.cn (F. Qian)

Abstract

Fluid catalytic cracking unit (FCCU) is an important refinery process by cracking heavy hydrocarbons to form lighter valuable products, including gasoline and diesel oil. However, the FCCU also generates the largest amount of CO_2 emissions among all the refinery units. To solve this problem, solvent-based carbon capture can be introduced to capture CO_2 in the flue gas from FCCU, but the energy consumption from the reboiler of the carbon capture plant will undoubtedly reduce the economic benefits of the refinery. In this paper, solvent-based carbon capture for an FCCU in a real life refinery is studied through process simulation. This study takes into account the process design and heat integration. An industrial FCCU with a feed capacity of over 1.4 million tons vacuum gas oil per year was modelled, and the process model was validated according to industrial operating data. A carbon capture plant model with MEA solvent was also developed in Aspen Plus® at pilot scale, and scaled up to match the capacity of the FCC unit. Case studies were performed to analyze the integration of the FCCU with commercial scale carbon capture plant, in which different heat integration options were discussed to reduce the energy consumption. The simulation results indicated that a proper design of heat integration will significantly reduce the energy consumption when the carbon capture plant is integrated with an industrial FCCU.

Keywords: Refinery; FCCU; Solvent-based carbon capture; Process simulation; Scale-up; Process analysis

1. INTRODUCTION

1.1. Background

The emissions of CO_2, known as one of major greenhouse gases, has a significant impact on the global warming and climate change. As a result of the world industry development, CO_2 emissions keep increasing rapidly in the last two centuries. It is reported that if no action is taken to reduce the atmospheric concentration of CO_2, it will rise to above 750 (*ppmv*) by 2100 [1]. As a response, the intergovernmental Panel on Climate Change (IPCC) indicated that CO_2 emissions need to be cut by a minimum of 50% to limit the average global temperature increment to 2℃ in 2050 [2-4].

Fluid catalytic cracking unit (FCCU), known as the heart of the refinery by cracking heavy hydrocarbons to form lighter valuable products, on the other hand, generates the largest amount of CO_2 emissions among all the refinery units, about 20-30% of total CO_2 emissions from a typical refinery [5]. Therefore, capturing CO_2 from FCCU flue gas will be an important step in reducing the total CO_2 emissions from the refinery.

In an industrial FCCU, most CO_2 is released from its regenerator, which is a coke combustion process. Therefore, several carbon capture technologies such as oxy-firing, pre-combustion and post-combustion carbon capture, could be applied to abate the CO_2 emissions [6]. Among them, the solvent-based post-combustion carbon capture (PCC), which commonly uses monoethanolamine (MEA) as the solvent, is the most promising and mature one. Compared with other technologies, it requires minimal modifications to FCCU, and has the most implementation cases in industry [7, 8]. Therefore, the solvent-based carbon capture with MEA is applied in this research.

1.2. Previous research

Solvent-based carbon capture has been studied by many researchers. Lawal et al. and Zhang et al.

proposed rigorous plant models respectively, and validated the models according to operating data from pilot plants [9, 10]. Lawal et al. also analyzed different modelling methods, which showed that rate-based modelling for PCC process is more accurate than equilibrium-based model [11, 12]. Considering the high heat duty in the reboiler of PCC stripper will bring a significate energy penalty for commercial implementation, Wang et al. indicated that the energy consumption can be reduced by better process integration [6]. Liu et al. simulated the heat integration of a 600MW_e supercritical coal-fired power plant (CFPP) with PCC process, and several integration cases were analyzed accounting for energy from different positions of the CFPP [13]. Roberto et al. deployed a commercial scale carbon capture plant for a 250MW_e combined cycle gas turbine (CCGT) power plant, and proposed exhaust gas recirculation to reduce penalty on thermal efficiency [14]. Luo et al. firstly studied on applying solvent-based carbon capture for cargo ships, and the cost degrees for the deployment were evaluated in different integration options [15].

The FCCU has also been widely investigated [16-19]. For the modeling of reaction kinetics, several methods were proposed by classifying the kinetics into different chemical lumps [20-23]. Among them, Aspen HYSYS®, a commonly used chemical engineering software, has also developed a 21-lump model to address heavier and more aromatic feeds [24, 25]. Flue gas from FCCU was analyzed by Fernandes et al. in detail, which indicated that the flue gas from FCCU regenerator contained a higher CO_2 concentration compared with flue gas from power plants [26]. In industry, considering the fact that the temperature of flue gas released from the FCCU regenerator is quite high (usually over 900K), waste heat recovery is therefore an effective way to promote the economic benefits. In this area, Johansson et al. analyzed the excess heat in the view of a whole refinery [27]. Al-Riyami et al. discussed the heat integration of a heat exchanger network for the FCC plant, in which the energy

efficiency and economic benefits were taken into account for estimating different heat integration options [28].

For the integration of FCCU with carbon capture plant, de Mello et al. deployed oxy-combustion technology for FCCU in large pilot scale to reduce CO_2 emissions [29]. Furthermore, de Mello et al. also compared the CO_2 capture performance between oxy-firing technology and solvent-based carbon capture for the FCCU at pilot scale, and concluded that oxy-firing concept would be an adequate technology for FCCU if ignoring the total capital cost and consequently FCCU modifications [30].

1.3. Motivation and novel contributions of this work

From the previous studies reviewed in Section 1.2, it can be observed that the deployments of solvent-based carbon capture plant have been mainly focused on the power plants. To the best of our knowledge, few papers studied the integration of solvent-based carbon capture with FCCU for the industrial scale. Flue gas from an industrial FCCU, different from that in power plants, contains more CO_2 and O_2 so that the size of capture plant should be redesign to meet these requirements. Furthermore, considering the large amount of excess heat in FCCU, heat integration should also be analyzed to compensate the energy penalty from carbon capture plants.

In summary, considering the mentioned problems, the novel contributions of this research are listed as follow:

(1) A steady state model for FCCU is developed, the parameters of which are calibrated based on operating data from real industry;

(2) Detailed study on scale-up of the solvent-based carbon capture process is discussed to match the flue gas requirements of the industrial FCCU;

(3) Case studies are performed to compare the performance of deploying solvent-based carbon

capture for FCCU with different heat integration options (in order to reduce energy consumption used for carbon capture).

1.4. Outline of this paper

This paper is organized as follows: the model development of the industrial FCCU is introduced and the model is also validated in Section 2. Section 3 describes the model development of the solvent-based carbon capture plant. In Section 4, the process model integration is presented, including flue gas pre-processing, model interface, and scale-up of the capture plant model. In Section 5, two case studies are performed to test the performance of the carbon capture deployment. Conclusions were drawn in Section 6.

2. Model development of the FCCU

2.1 FCCU process description

The reference plant selected in this work is an industrial UOP FCC unit in a Sinopec oil refinery with a feed capacity of over 1.4 million tons vacuum gas oil (VGO) per year. The unit has two major components: riser and regenerator. The simplified flow diagram of the FCCU is illustrated in Fig. 1.

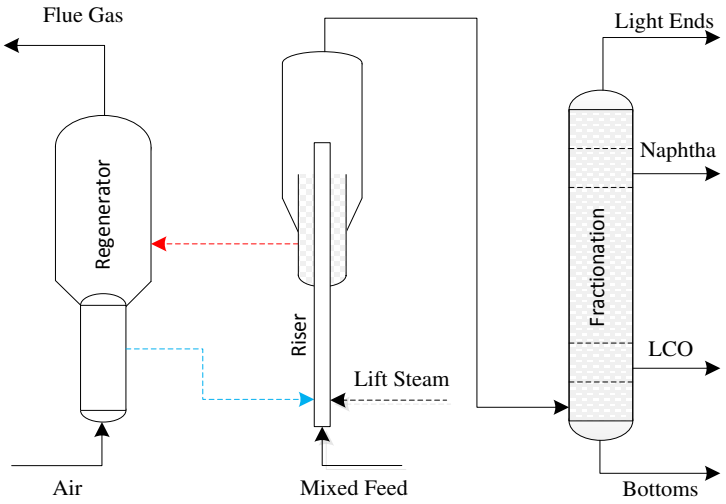

Fig. 1. Simplified flow diagram of the FCCU in refinery.

As presented in Fig. 1, the riser is the main reactor where most cracking reactions occur. As all the reactions are endothermic, the feedstock, before entering the riser, should be preheated to around 533-644K by the feed preheat system. The preheated feed then comes in contact with a hot fluidized catalyst (over 811K) in the riser, and the components of the feed undergo several reactions on the catalyst surface. After that, the effluent from the riser is sent to the fractionator for the separation of liquid and the gaseous products.

The spent catalyst, on the other hand, is sent to the regenerator, which is another major component in FCCU. It is used to remove coke on the catalyst surface by combustion with air so as to maintain the activity of the catalysts, and also supply heat to the riser. To reactivate the catalyst, coke is burned off in the regenerator by operating at about 988K and about 2.41 bar. In addition, a large amount of flue gas (flow rate over 30kg/s) at high temperature is produced because of the combustion in the regenerator of FCCU [28].

2.2 Model development for the FCCU

Complex reaction kinetics are involved in FCCU modeling, which requires a proper reaction lump network and accurate thermodynamics. In addition, the integration of the FCCU with solvent-based carbon capture is to be considered in this work, the process model should also be able to describe the flue gas accurately (including flow rate, chemical compositions, pressure and temperature). Therefore, the Aspen HYSYS/Petroleum Refining FCCU model is applied in this research. It relies on a series of sub-models that can simulate an entire operating unit while satisfying the riser and regenerator heat balance. The main sections of the mentioned FCCU model is summarized in Table 1, for the detailed information, readers can refer to ref [31].

Table 1. Brief summary of Aspen HYSYS/Petroleum Refining FCC sub-models [31]

Submodel	Purpose	unit operation
riser	convert feed to product species using 21 lump kinetics	modified plug-flow reactor
reactor/stripper	complete feed conversion and remove adsorbed hydrocarbons	bubbling-bed reactor with two phases
regenerator	combust coke present on the catalyst	bubbling-bed reactor with two phases
delumper	convert lumped composition into a set of true boiling point (TBP) pseudo-components suitable for fractionation	

As listed in Table 1, the riser has been modeled with a plug-flow reactor (PFR) under pseudo-steady conditions. In the riser, the vapor hydrocarbon cracks on the solid catalyst surface. As cracking reactions involve large amount of species, it will be too complex to simulate each specie in the process model. Thus, a 21 lump kinetics reaction network is applied to deal with this complexity. All the species are represented by the 21 components as listed in Table 2. Furthermore, as the 21-lump model includes discrete lumps for the kinetic and metal coke, a coke-on-catalyst approach is used to model catalyst deactivation. In addition, a rate equation in the kinetic network for coke balance is also involved on the catalyst, which is formulated as follow [17]

$$\begin{aligned}\phi_{coke} &= \phi_{KCOKE}\phi_{MCOKE} \\ &= \exp(-a_{KCOKE}C_{KCOKE})\exp(-a_{MCOKE}C_{MCOKE}f(C_{METALS}))\end{aligned} \tag{1}$$

Where a_{KCOKE} is the activity factor kinetic coke, a_{MCOKE} is the activity factor for metal coke, C_{KCOKE} is the concentration of kinetic coke on the catalyst, C_{MCOKE} is the concentration of metal coke on the catalyst, and C_{METALS} represents the concentration of metals on catalyst.

Table 2. Summary of 21-lump kinetics (refer to [31])

boiling point range	Lumps
<C5	light gas lump
C5 to 221℃	Gasoline
221-343℃	light paraffin (PL)
(VGO)	light naphthene (NL)
	light aromatics with side chains (Als)
	one-ring light aromatics (ALr1)
	two-ring light aromatics (ALr2)
343-510℃	heavy paraffin (PH)

(heavy VGO)	heavy naphthene (NH)
	heavy aromatics with side chains (AHs)
	one-ring heavy aromatics (AHr1)
	two-ring heavy aromatics (AHr2)
	three-ring heavy aromatics (AHr3)
Over 510℃	residue paraffin (PR)
(residue)	residue naphthene (NP)
	residue aromatics with side chains (Ars)
	one-ring residue aromatics (ARr1)
	two-ring residue aromatics (ARr2)
	three-ring residue aromatics (ARr3)
coke	kinetic coke (produced by reaction scheme)
	metal coke (produced by metal activity on the catalyst)

The regenerator is modelled by two separate phases, the dense phase and the dilute phase. The former is the bottom part of the regenerator where it is highly concentrated with catalyst, and the latter is the top part of the regenerator which contains a negligible amount of catalyst particles. Therefore, the regenerator is modelled as a bubbling-bed reactor with two phases.

2.3 Model validation

The proposed steady state model for FCCU is validated by mean values of industrial operating data. These data are collected over 30 days in a relative steady operating conditions. Table 3 gives the industrial operating conditions and the model predicted values in comparison with those data obtained from industry.

Table 3. Validation results of the FCCU model

Variable	unit	Value
Fresh feed flow rate	*t/h*	150.74
Fresh feed temperature	*K*	496.87
Fresh feed pressure	*kPa*	244.44
Steam flow rate	*t/h*	9.10
Steam temperature	*K*	640.90
Steam Pressure	*kPa*	0.97
Riser outlet temperature	*K*	783.84
Dense Bed Temperature	*K*	967.86
Air Volume Flow	Nm^3/h	90000.00

Reactor Pressure	*kPa*	173.24		
Regenerator - Reactor Pressure Difference	*kPa*	22.49		
		Model prediction	Industry Data	Relative Error
Gas (C1, C2)	*t/h*	2.96	4.91	65.97%
LPG	*t/h*	20.41	19.50	4.45%
Gasoline	*t/h*	73.96	74.36	0.55%
Diesel Oil	*t/h*	36.40	34.95	3.99%
O_2 and Ar (in flue gas)	*wt%*	5.20	5.25	0.90%
CO_2 (in flue gas)	*wt%*	12.78	13.32	4.23%
CO (in flue gas)	*wt%*	0	0	

As shown in Table 3, the relative error of gasoline and diesel oil, which are the main products of the FCCU, are all below 4%. Meanwhile, the proposed FCCU model also shows a good performance in predicting the flue gas compositions, as the relative error of O_2 and CO_2 concentration are 0.9% and 4.23% respectively. It can also be observed that the error of GAS in products is as high as 65.97%. In fact, as GAS is a by-product for the FCCU and the mass flow rate is relatively small compared with the main products, the predicting error of GAS is also acceptable. Thus, it can be concluded that the proposed FCCU model is suitable for the following study on the model integration between the FCCU and the carbon capture plant. Furthermore, the model predicted flue gas compositions and flow rate are also listed in Table 4.

Table 4. Flue gas composition and mass flow rate

	Unit	Flue gas
O_2	*wt%*	4.20
N_2	*wt%*	82.02
CO_2	*wt%*	12.78
CO	*wt%*	0.00
Ar	*wt%*	1.00
Temperature	*K*	993.07
Flow rate	*kg/s*	30.304

3. Model development of solvent–based carbon capture plant using MEA

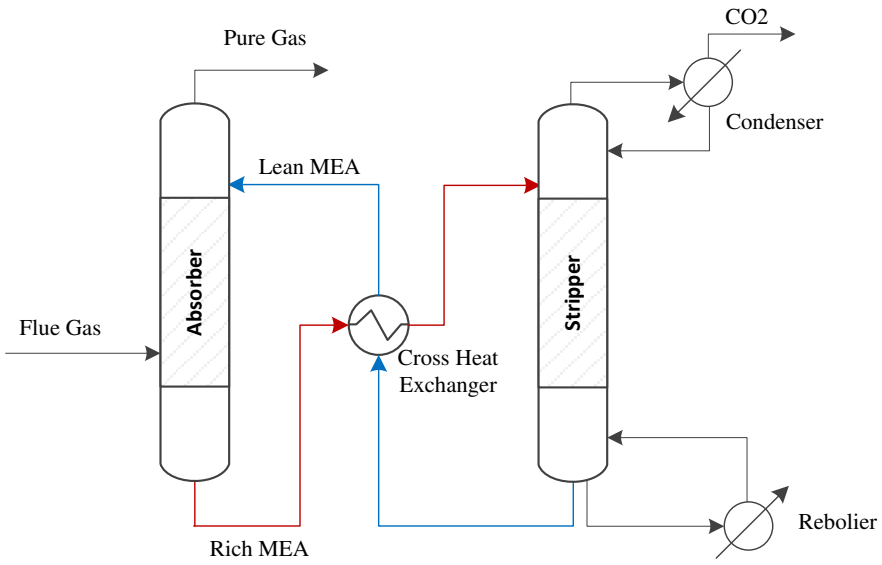

Fig. 2. Simplified flow diagram of the carbon capture plant with MEA solvent [9, 11, 12].

3.1. Solvent-based carbon capture plant description

As shown in Fig. 2, a typical carbon capture plant with MEA solvent can be described as follow. Firstly, the pre-processed flue gas is sent to the bottom of the absorber, where most of the CO_2 in the flue gas is chemically absorbed by the lean MEA solvent, and the scrubbed gas is released from the top. The rich solvent is then heated in a cross heat exchanger and pumped into the stripper. The stripper, on the contrary, is a place where CO_2 is extracted from the rich solvent and collected with a high purity. At the same time, the regenerated solvent is pumped back to the absorber as the lean solvent through the cross heat exchanger to reduce the temperature. In the capture plant, the main energy consumption is the reboiler heat duty of the stripper. To describe the absorption performance of the process, several technical terms are defined as follows.

CO_2 loading

$$CO_2\ loading\ (mol\,CO_2/mol\,MEA) = \frac{[CO_2]+[HCO_3]+[CO_3^{2-}]+[MEACOO^-]}{[MEA]+[MEA^+]+[MEACOO^-]} \quad (2)$$

Specific duty

$$Q_{spe}(GJ/tonCO_2) = \frac{Q_{reb}}{F_{CO_2,cap}} \quad (3)$$

In this work, the capture plant model we developed is based on the operating data from a pilot plant at the University of Texas, Austin [32]. The pilot plant is a closed-loop absorption and stripping facility as described above, where both the absorber and regenerator are 0.427m in diameter and packed with two sections of 3.05m packing. The MEA concentration in the lean solvent is 32.5wt%. The absorber is operated at atmospheric pressure with a random metal packing, IMTP no. 40, while the stripper is operated at a pressure of 1.7 bar and filled with a structured packing, Flexi Pac1Y [32].

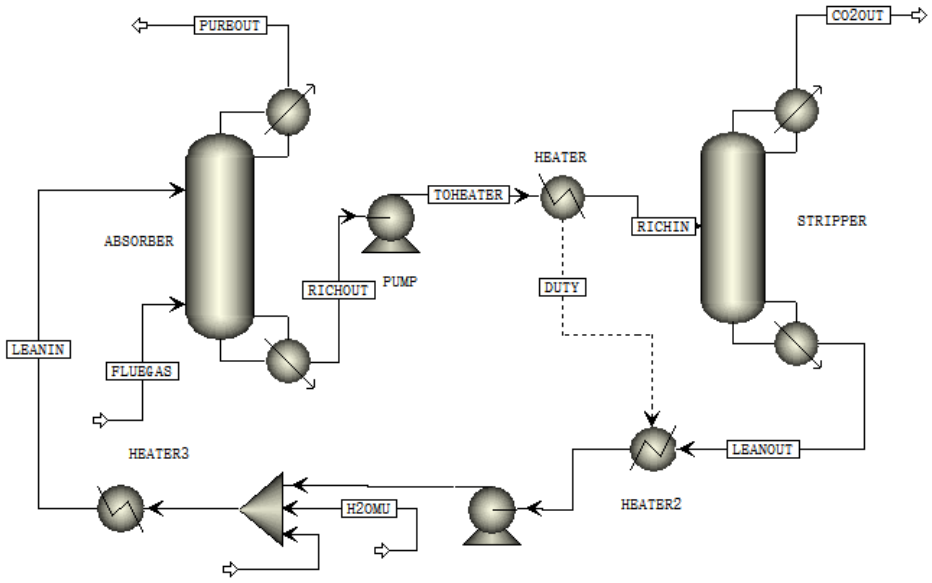

Fig. 3. Flowsheet of the carbon capture plant model in Aspen Plus®.

3.2 Model development of the capture plant

The capture plant model has been developed in Aspen Plus®, which is shown as Fig. 3. Both the absorber and stripper are modeled using the rate-based model, which has been proved to have a better accuracy than an equilibrium model.

For the physical property method, the Electrolyte Non-Random-Two-Liquid (ELECNRTL) model is selected for liquid, and RK equation of state for vapor [14]. Meanwhile, for the reaction kinetics,

both equilibrium and rate-controlled reactions are used, and the kinetic models proposed by Aboudehir et al., and Aspentech were selected in this study, which are defined as follow [33, 34]

The equilibrium reactions

$$2H_2O \leftrightarrow H_3O^+ + OH^- \quad (4)$$

$$HCO_3^- + H_2O \leftrightarrow H_3O^+ + CO_3^{2-} \quad (5)$$

$$MEAH^+ + H_2O \leftrightarrow MEA + H_3O^+ \quad (6)$$

The rate-controlled reactions

$$CO_2 + OH^- \rightarrow HCO_3^- \quad (7)$$

$$HCO_3^- \rightarrow CO_2 + OH^- \quad (8)$$

$$MEA + CO_2 + H_2O \rightarrow MEACOO^-H_3O^+ \quad (9)$$

$$MEACOO^- + H_3O^+ \rightarrow MEA + CO_2 + H_2O \quad (10)$$

The equilibrium constants K_{eq} for the reactions (4) to (6), on a molar concentration basis, can be determined as

$$\ln(K_{eq}) = A + \frac{B}{T} + C \cdot \ln(T) + D \cdot T \quad (11)$$

The kinetic expressions (7) to (10) are governed by the power law expression

$$r = kT^n \exp(-\frac{E}{RT}) \prod_{i=1}^{N} C_i^{a_i} \quad (12)$$

The values of the parameters A, B, C and D for the equilibrium reactions as well as the kinetic parameters are given in Table 5.

The packing section of the absorber and stripper are specified with the same type of packing and with the same dimensions as the pilot plant. Readers can refer to studies [16, 32] for more details about the development of the absorber and stripper models.

Table 5. Coefficient of equilibrium constants and kinetic parameters

Equation no.	A	B	C	D
1	132.889	-13455.9	-22.477	0
2	216.049	-12431.7	-35.482	0
3	-3.038	-7008.357	0	-0.003
	k		E (cal/mol)	
4	4.32E+13		13249	
5	2.381E+17		28451	
6	5.30E+10		9855.8	
7	2.183E+18		14138.4	

3.3 Model validation

The accuracy of the proposed carbon capture plant model is validated by operating data from the same pilot plant which our plant model is based on. The operating data were collected from 48 experimental cases with different operation conditions in a test campaign [32]. Among the 48 experimental cases, Case 28 has relatively high liquid to gas (L/G) ratio and CO_2 capture level, while the liquid to gas (L/G) ratio and CO_2 capture level of Case 47 are much lower. These two cases were selected to test the performance of the proposed capture plant model with different operating conditions. The detailed information of the operating data are listed in Table 6.

Figs. 4 and 5 show the validation results for the absorber and stripper temperature profiles of Cases 28 and 47 respectively, where solid blue line indicates the model predicted data, and 'x' represents the operating data from pilot plant. It can be seen from the figures that the solid lines are very close to the 'x' points, which shows that the developed model has selected proper physical properties and reaction kinetics to reflect the internal changes of the peaking columns. In Table 7, the simulation results are also compared with model from Canepa et al. [14], which has shown a good predicting accuracy. It can be observed that model in this work shows a better performance in predicting rich loading value. Thus, it can be concluded that, with different liquid to gas (L/G) ratios, the proposed solvent-based

carbon capture plant model has a good predicting performance. Therefore, the proposed capture plant model is suitable for the integration of the FCCU with the carbon capture plant.

Table 6. Process conditions for experimental Case 28 and Case 47 [32]

	unit	Case 28	Case 47
Lean in flow rate	*L/min*	81.92	30.13
Lean in temperature	*K*	313.14	313.32
Flue gas flow rate	m^3/min	11.00	8.22
Flue gas temperature	*K*	321.08	332.38
Flue gas pressure	*kPa*	105.19	103.32
Flue gas CO_2 content	*mol%*	16.54	18.41
Regenerator pressure	*kPa*	162.09	68.95
Regenerator temperature	*K*	345.21	354.33
Condenser temperature	*K*	287.79	297.14
Reboiler temperature	*K*	388.05	366.30

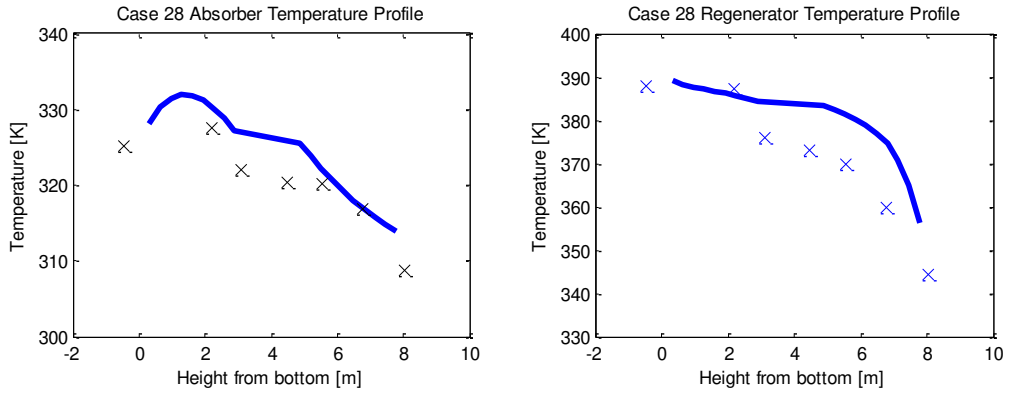

Fig. 4. Temperature profile for Case 28 (solid blue lines represent model predictions while '×' represents experimental data).

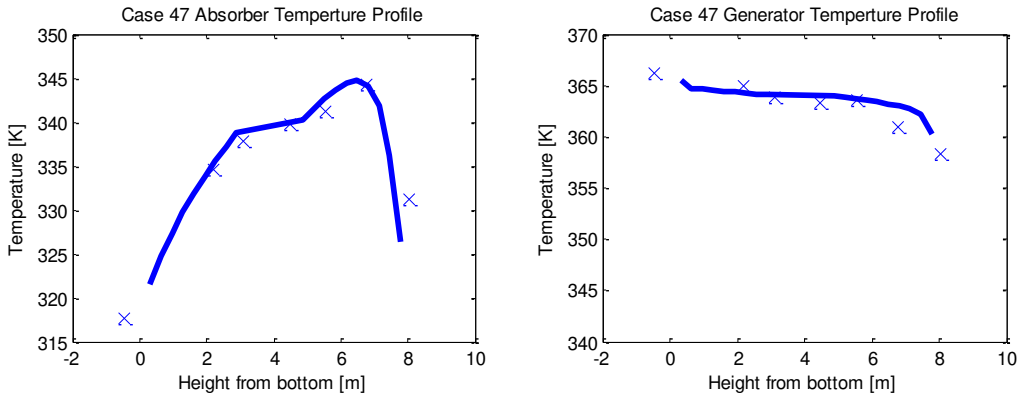

Fig. 5. Temperature profile for Case 47 (solid blue lines represent model predictions while '×' represents experimental data).

Table 7. Capture plant performance for Case 28 and Case 47

	Unit		Case 28	Case 47
lean loading	*mol* CO_2/*mol* MEA	Experimental	0.287	0.281
rich loading	*mol* CO_2/*mol* MEA	Experimental	0.412	0.539
		This work	0.405	0.487
		Canepa et al. [14] model	0.409	0.467
CO2 capture level	%	Experimental	86	69
		This work	72.34	58.94
		Canepa et al. [14] model	71	68.7

4. Integration of the FCCU with carbon capture plant

Both FCCU model and solvent-based carbon capture plant model have been described in Sections 2 and 3 respectively. But, in fact, the flue gas released from the FCCU cannot be sent to the capture plant directly. Before integrating the two process models, several problems should be discussed first.

4.1 Flue gas pre-processing

For the industrial FCCU in refinery, the generated flue gas will go through a series of energy recovery equipment before entering chimney. A simplified diagram of the flue gas flow from the reference industrial FCCU to chimney is shown in Fig. 6. Firstly, as the flue gas at the outlet of the FCCU has a very high temperature (around 992K in Fig. 6), which means that it is the highest in heat grade, this part of energy is generally recovered by flue gas turbine to generate electric power. Then, the flue gas with temperature decreased to around 759K, enters the waste heat steam generator (WHSG) to achieve further heat recovery. Finally, the flue gas temperature drops to around 453K, and released through chimney.

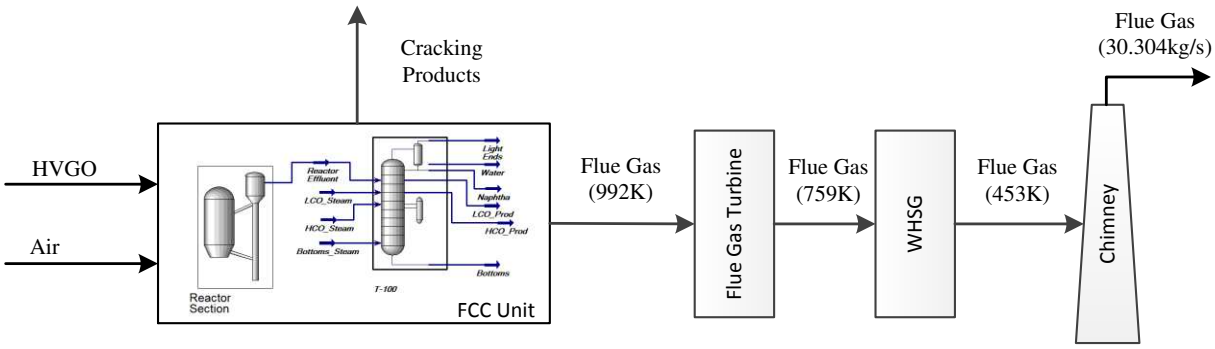

Fig. 6. Process diagram of the reference industrial FCCU (Reference case).

In this work, the flue gas from the outlet of the WHSG will be sent to a carbon capture plant, instead of being released through chimney directly. Before entering the absorber of the carbon capture plant, pre-processing should be done. First, the flue gas has to be cooled down to around 313-323K in order to improve the absorption efficiency and reduce solvent losses due to evaporation. The cooling system consists of direct contact cooler which is modelled as a two theoretical stages tower with Raschig rings packing. A spray of water at 298K has been used to cool down the flue gas to around 313K. The Aspen Plus® block RadFrac is used to fulfill this task [14].

Furthermore, acid gases, such as NO_x and SO_x, have to be taken out of the flue gas, as they tend to form teat stable salts that cannot be regenerated with the solvent, compromising its absorption capacity. This can be removed by either electrostatic precipitators or bag house filters. Oxygen content also has to be controlled to avoid corrosion of the equipment and solvent degradation. For simplicity, an ideal cleaning process has been considered and therefore all the unwanted species have been taken out, leaving a flue gas with only four species [14].

4.2 Interface of the FCCU model and carbon capture plant model

As the two models are developed in different software, where the FCCU is modeled in Aspen HYSYS®, and the capture plant is modeled in Aspen Plus®, data transmission should be realized. In

284 this work, an interface program is coded in Visual Basic to collect the model simulated flue gas
285 information in Aspen HYSYS® and transfer it to the Aspen Plus® model.

286 **4.3 Water balance**

287 In the solvent-based carbon capture plant, as the absorption reaction is exothermic, some water will
288 be evaporated with CO_2 being absorbed into the MEA solvent. In this model, this part of water will be
289 released with the pure flue gas from top of the absorber. Thus, the water balance cannot be maintained
290 because of the capture plant model is a closed-loop system. This problem was also discussed by Lawal
291 et al. [9] and Canepa et al. [14] when dealing with flue gas from different power plants.

292 In this study, as less water contained in the flue gas from FCCU, the water balance issue should also
293 be taken into account. Therefore, a make-up water stream is added into the capture plant model to
294 compensate the water loss. The flowrate of the make-up water is determined according to the operating
295 conditions of the capture plant.

296 **4.4 Scale-up of the solvent-based carbon capture process**

297 The model scale-up is a key step for the integrating simulation, the aim of which is to redesign the
298 size of the capture plant model to match the requirements of the flue gas from FCCU. It includes the
299 design of the number and size of the absorber and stripper, as well as the solvent flow rate. In this
300 work, the following assumptions should be taken into account:

301 (a) Solvent is 32.5*wt*% MEA;

302 (b) 90% capture level;

303 (c) The same operating pressure for absorber and regenerator in the pilot plant will be used at full scale
304 (i.e. 1 and 1.6 bar, respectively);

305 (d) Adiabatic absorption process;

306 (e) Acid gases have been removed from the flue gas;

307 (f) No water wash section in the absorber.

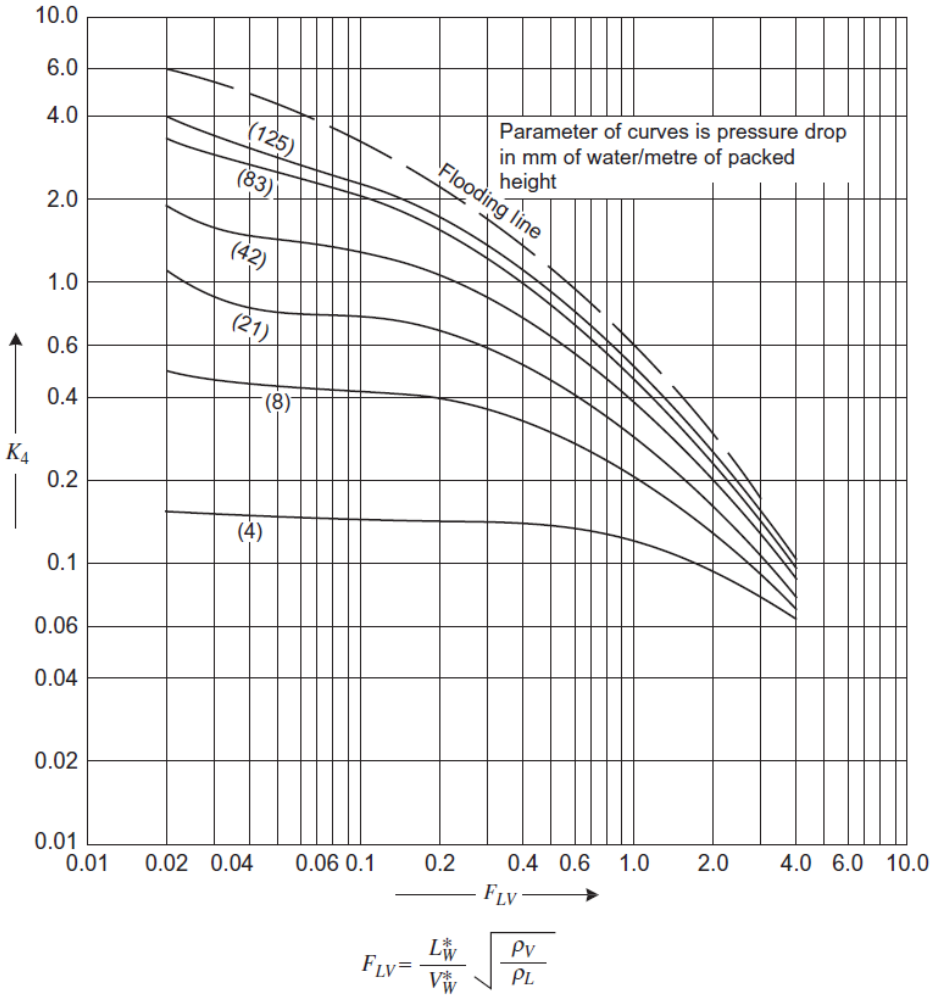

308

309 Fig. 7. Generalized pressure drop correlation, adapted from a figure by Koch-Glitsch, LP, with

310 permission (This figure was published in [35]).

311 For scale-up, it is important to calculate the cross-sectional areas of absorber and stripper. The

312 methodology is adopted from [14]. For the absorber, given the flus gas mass composition and flow

313 rate in Table 4 and assuming capture level of 90%, and the MEA solvent absorption capacity is 0.18

314 mol CO_2/mol MEA. Thus, the required solvent mass flow rate is calculated to be 82.63kg/s (with

315 32.5*wt*% MEA).

316 Then, the required column diameter can be estimated through a generalized pressure drop correlation
317 (GPDC) given by Sinnot [35]. As shown in Fig. 7, with the lines of constant pressure drop as a
318 parameter, the relationship between the flow parameter F_{LV} and the modified gas load K_4 is given, and
319 both of the terms are defined respectively as follow

320 $$F_{LV} = \frac{L_w^*}{V_w^*}\sqrt{\frac{\rho_V}{\rho_L}} \tag{13}$$

321 $$K_4 = \frac{13.1(V_w^*)^2 F_p(\mu_L/\rho_L)^{0.1}}{\rho_V(\rho_L - \rho_V)} \tag{14}$$

322 Where, F_{LV} = the flow parameter which is related to *L/G* ratio;

323 K_4 = a modified gas load;

324 F_p = packing factor, characteristic of the size and type of packing, m^{-1};

325 V_w^* = vapor mass flow rate per unit cross-sectional area, $kg/m^2 s$;

326 μ_L = liquid viscosity, Ns/m^2;

327 ρ_L, ρ_v = liquid and vapor densities, kg/m^3.

328 In engineering practice, the column will be designed to operate at the highest economical pressure drop,
329 to ensure good liquid and gas distribution. A recommended value for the absorber and stripper is
330 between 15 to 50 mm H_2O per meter packing. In this paper, the pressure drop of 42 mm H_2O per meter
331 packing is selected for the scale-up. It can be observed from Equations (13) and (14) that once the
332 liquid and gas flow ratio and ρ_L, ρ_v are given, the term F_{LV} can be calculated. Then, with the
333 assumed pressure drop, the gas load K_4 can be estimated from Fig. 7. From Equation (14), the gas mass
334 flow rate per unit column cross-sectional area is obtained. The total area required can be evaluated
335 given the flue gas flow rate that has to be processed.

The same procedure was adopted for the scale-up of stripper. The liquid flow is equal to the sum of the rich solvent mass flow rate plus the reflux rate while the gas flow is equal to the boiled-up rate. The adopted values as well as the obtained results are presented in Table 8.

Table 8. Sizing first guess solution: Assumption and results

Assumptions	unit	Absorber	Stripper
L_w*/V_w*		2.73	12.67
p_v	kg/m^3	1.364	1.022
p_L	kg/m^3	1084.01	1023.69
Pressure drop	*mm H2O/packing*	42	42
F_p	*L/m*	78.74	168.2
u_L	*Pa S*	0.00355	0.000969
F_{LV}		0.097	0.403
K_4		1.4	0.7
Cross section area required	m^2	11.38	6.09
diameter required	*m*	3.81	2.78

A first guess diameter of the absorber and stripper has been estimated according to the methods mentioned above. The information of the scaled up capture plant model is listed in Table 9. The estimated sizing values have been simulated with the previously developed model for capture plant in Aspen Plus®. In the simulation, lean loading is an important value that influences the reboiler duty of the stripper. In this work, lean loading of 0.30 *mol* CO_2/ MEA is selected to deal with 12.78wt% CO_2 concentration in the flue gas, which is a relatively high value compared with that in the power plants. The overall performance of the scaled up capture plant is shown in Table 10.

Table 9. Capture plant equipment design

	unit	Absorber	Stripper
Column number		1	1
Column packing		IMTP no.40	Flexipack 1 Y
Column diameter	*m*	3.81	2.78

Column packing height	*m*	30	30
Column pressure	*kPa*	101	162

348 Table 10. The overall performance of the scaled up capture plant model

	unit	model scale up
Flue gas flow rate	*kg/s*	30.304
Flue gas CO_2 content	*wt%*	12.78
Solvent MEA content	*wt%*	32.50
Capture level	*%*	90
CO_2 captured	*kg/s*	3.491
L/G ratio	*kg/kg*	2.507
Lean loading	*mol* CO_2*/mol* MEA	0.30
Rich loading	*mol* CO_2*/mol* MEA	0.496
Stripper heat duty	*MW*	14.677
Specific duty	*GJ/ton* CO_2	4.204

349 # 5. Case studies and discussions

350 Three case studies are presented to test the performance of the integration of the industrial FCCU
351 with solvent-based carbon capture. As introduced in Fig. 6, excess heat from the reference FCCU can
352 be summarized as: (1) excess heat entering chimney. As the flue gas temperature entering chimney is
353 around 453K, while the stripper reboiler temperature is around 393K, energy from 453K to 403K, with
354 10K mean temperature difference, can be recovered to heat the stripper reboiler; (2) heat recovered by
355 WHSG; (3) heat used by Flue Gas Turbine; (4) refinery excess heat from steam network. Thus, case
356 studies are simulated and discussed with the consideration of different heat integration options.

357 ## 5.1 Justification of case studies

358 5.1.1 Case 1: Only FCC excess heat are supplied to the CO_2 capture process

359 In Case 1, the heat required by carbon capture plant is totally supplied by the excess heat of the
360 FCCU itself. Considering that electricity is more expensive, heat used by Flue Gas Turbine (i.e. (3)) is
361 still used for electricity generation. Therefore, only heat from (1) and (2) is used for carbon capture in

this case. To utilize this part of energy, modifications should be done for both FCCU and carbon capture plant. A heat exchanger is added to collect the excess energy from chimney. A multiple-shell kettle reboiler [36], which can mix energy from different sources, is equipped in the stripper of the carbon capture plant. The heat integration of Case 1 is illustrated in Fig. 8.

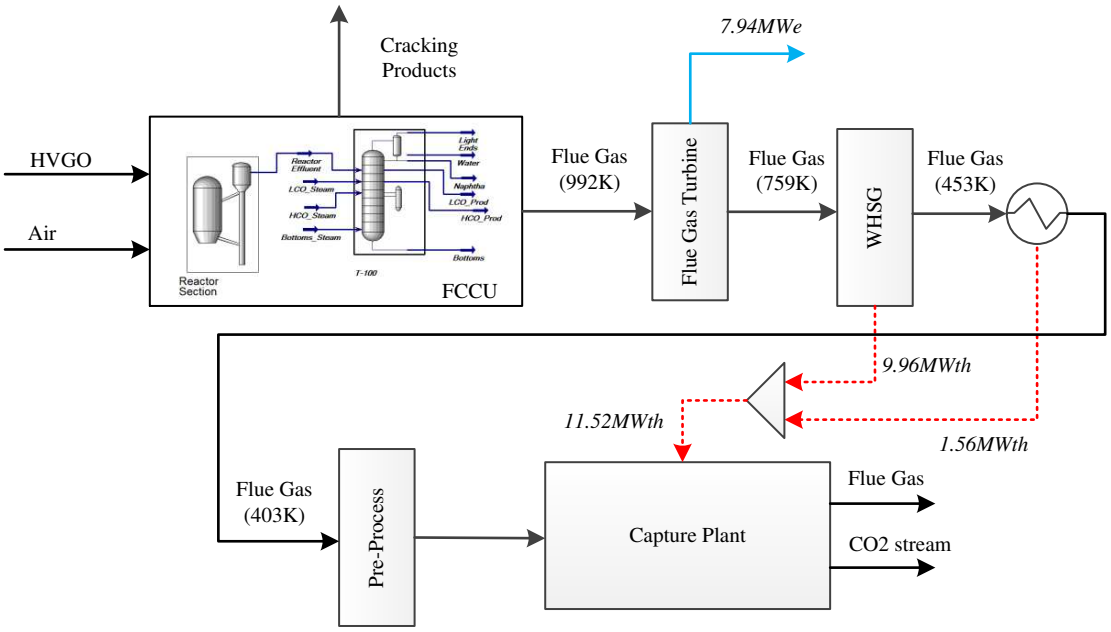

Fig. 8. Process diagram of Case 1.

5.1.2 Case 2: guarantee 90% CO_2 capture level with FCCU excess heat only

In this case, a 90% CO_2 capture level, which is the designed value of the solvent-based carbon capture plant, is attempted to guarantee. In this sense, part of energy in Flue Gas Turbine (i.e. (3)) should be used for carbon capture. As shown in Fig. 9, the outlet temperature of the Flue Gas Turbine is raised to 854.1K, which means that the amount of electricity generated from (3) is decreased. This part of heat is added to the WHSG to guarantee the CO_2 capture level.

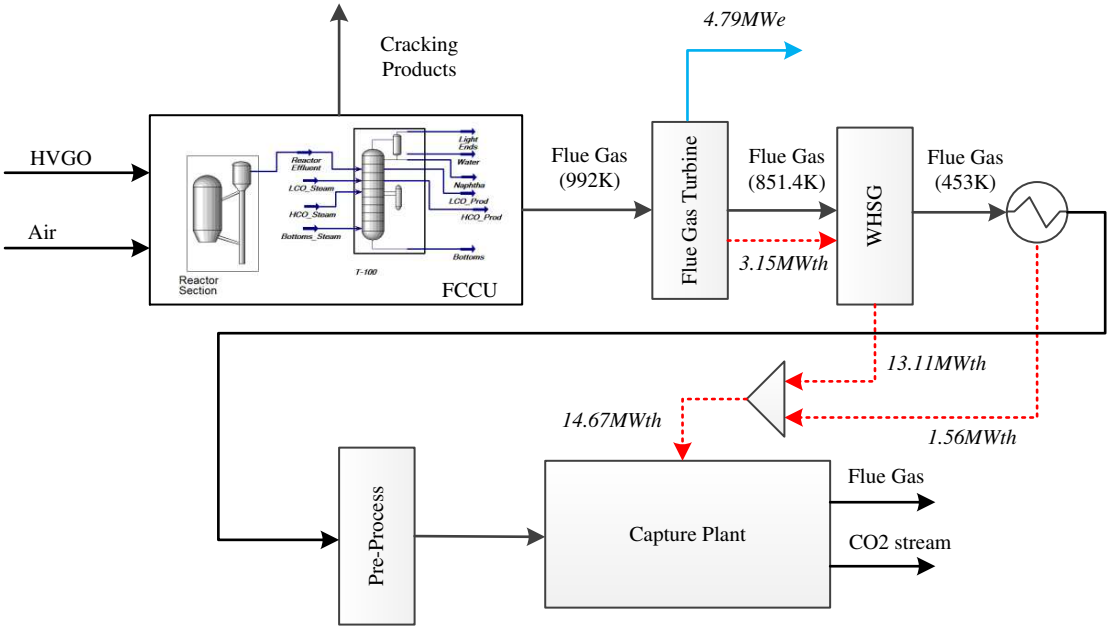

Fig. 9. Process diagram of Case 2.

5.1.3 Case 3: guarantee 90% CO_2 capture level with additional heat supply

The aim of heat integration in this case is also to guarantee 90% CO_2 capture level. An additional heat supply from steam network (i.e. (4)) is introduced to replace the amount of heat taken from Flue Gas Turbine (i.e. (3)). In this way, electricity generated by Flue Gas Turbine will not be influenced. In refinery, the steam network is used to collect the excess energy from different units and supply heat to the carbon capture plant. The process diagram of this case is shown in Fig. 10.

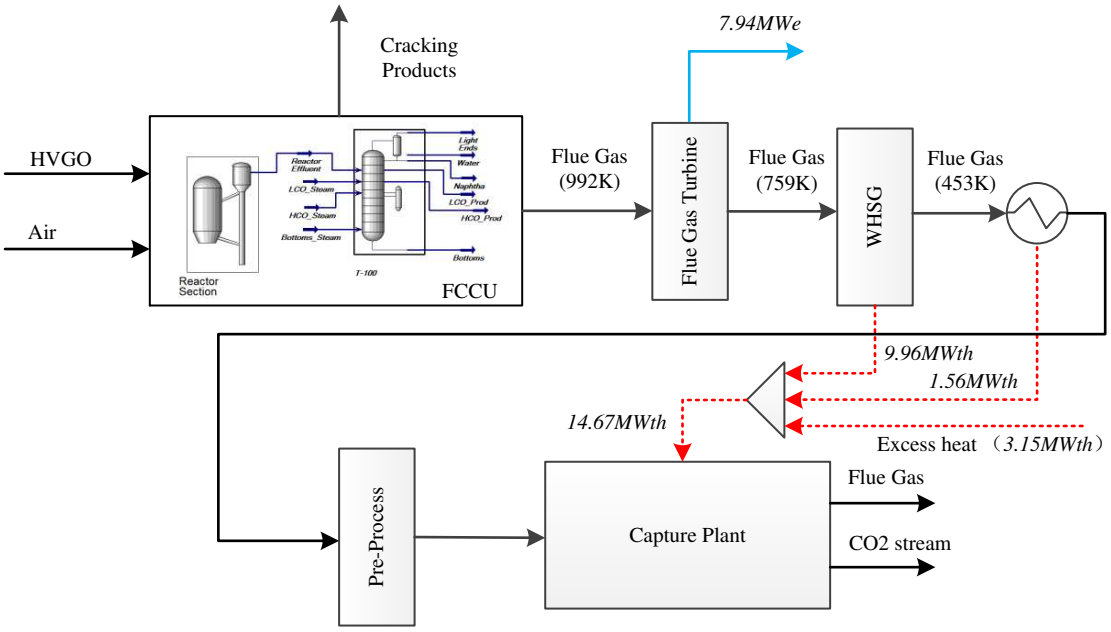

Fig. 10. Process diagram of Case 3.

5.2 Results and discussion

The results of all the three case studies are listed in Table 10. In Case 1, considering the flue gas temperature reduced from 759K to 453K (previously used by WHSG), 9.96MW_{th} heat can be provided to the carbon capture stripper reboiler. Furthermore, the energy in (1) collected by heat exchanger is 1.56MW_{th}. These two parts of heat are mixed by the multiple-shell kettle reboiler. As a result, 78.02% CO_2 in flue gas can be captured through this heat integration option. In fact, as the designed capture level is 90%, Case 1 cannot support the capture plant to reach that value. In summary, using the excess heat in the FCCU alone needs the minimal process modification for the industrial FCCU, but at the cost of reducing CO_2 capture level.

In Case 2, the inlet temperature of WHSG is raised to 851K, which enables WHSG to collect more heat, as high as 13.11MWth as shown in Fig. 9. It can be observed from Table 10 that the electricity generated by the Flue Gas Turbine will decrease, from 7.94MW_e to 4.79MW_e as shown in Fig. 9. Compared with the reference case, the electricity power decreased by 39.67%. However, the CO_2

capture level reaches 90%.

In Case 3, the capture plant needs no energy from the Flue Gas Turbine any more. Instead, this part of energy is replaced by excess heat from refinery steam network. It can be seen from Fig. 10, the inlet and outlet temperatures of the Flue Gas Turbine keep the same as the reference case, which means that the electricity generated by Flue Gas Turbine will not be affected. Besides, an additional heat stream is equipped to supply the excess heat from refinery. With the help of multiple-shell kettle reboiler, three heat streams from different sources are mixed to maintain 90% capture level of the capture plant.

Table 10. Summary of the results of the three case studies

	Unit	Ref Case	Case 1	Case 2	Case 3
Flue gas flow rate	*kg/s*	30.300	30.300	30.300	30.300
Flue gas CO_2 content	*mol%*	12.780	12.780	12.780	12.780
Solvent MEA content	*wt%*	32.500	32.500	32.500	32.500
Capture level	*%*	90.000	78.021	90.049	90.000
CO_2 captured	*kg/s*	3.490	3.030	3.490	3.490
L/G ratio	*kg/kg*	2.492	1.989	2.492	2.492
Lean loading	*mol* CO_2*/mol* MEA	0.300	0.300	0.300	0.300
Rich loading	*mol* CO_2*/mol* MEA	0.500	0.515	0.497	0.497
WHSG	*MW*	9.960	-	-	-
Electric power	*MW*	8.080	8.080	4.920	8.080
Steam network energy	*MW*	0.000	0.000	0.000	3.150
Stripper heat duty	*MW*	14.671	11.533	14.671	14.671
Specific duty	*GJ/ton* CO_2	4.200	3.803	4.200	4.200
Make up water	*kg/s*	3.037	3.068	3.037	3.037

6. Conclusions

The integration of an industrial FCCU with solvent-based carbon capture was investigated through process simulation in this work. A steady state model for FCCU was developed using Aspen HYSYS/Petroleum Refining sub-models, and validated based on operating data from a real life refinery in China. A steady state model for carbon capture plant with MEA solvent was also developed in Aspen Plus®. The model was validated with operating data from a pilot plant. For the process

integration, considering the CO_2 concentration and flow rate of the flue gas from FCCU, the capture plant model is scaled up, especially for the design of the diameter and height of the packed columns, to match the capacity of the FCCU.

Three case studies were performed to analyze the performance of deploying solvent-based capture plant for the industrial FCCU, in which different heat integration options were used to reduce the energy consumption of the capture plant. The simulation results presented in this paper indicated that a proper design of heat integration will significantly improve the carbon capture and save energy when the carbon capture plant is applied for an industrial FCCU.

Acknowledgement

The authors would like to acknowledge the financial support from EU FP7 Marie Curie International Research Staff Exchange Scheme (Ref: PIRSES-GA-2013-612230).

References

[1]. IPCC, Climate Change. Mitigation of climate change. UK: Cambridge University Press; 2014. P. 2015.

[2]. UNEP, 2005. United Nations Environment Programme, Introduction to Climate Change, http://www.grida.no/climate/vital/06.htm.

[3]. IPCC. Managing the risks of extreme events and disasters to advance climate change adaption. Cambridge (United Kingdom)/ New York (NY, USA): Cambridge University Press; 2012.

[4]. Deng F, Ma L, Gao X, et al. The MR-CA Models for Analysis of Pollution Sources and Prediction of PM2. 5. IEEE Transactions on Systems, Man, and Cybernetics: Systems, 2017.

[5]. Escudero AI, Espatolero S, Romeo LM. Oxy-combustion power plant integration in an oil refinery to reduce CO_2 emissions. Int. J Greenhouse Gas Control 2016; 45:118-129.

[6]. Wang M, Lawal A, Stephenson P, Sidders J, Ramshaw C. Post-combustion CO_2 capture with chemical absorption: A state-of-the-art review. Chemical Engineering Research and Design 2011; 89:1609-1624.

[7]. Luo X, Wang M. Improving prediction accuracy of a rate-based model of an MEA-based carbon capture process for large-scale commercial deployment. Engineering 2017; 3: 232-243.

[8]. Rochelle G T. Amine scrubbing for CO_2 capture. Science, 2009, 325(5948): 1652-1654.

[9]. Lawal A, Wang M, Stephenson P, et al. Dynamic modelling and analysis of post-combustion CO_2 chemical absorption process for coal-fired power plants. Fuel, 2010, 89(10): 2791-2801.

[10]. Zhang Y, Chen H, Chen C C, et al. Rate-based process modeling study of CO_2 capture with aqueous monoethanolamine solution. Industrial & engineering chemistry research, 2009, 48(20): 9233-9246.

445 [11]. Lawal A, Wang M, Stephenson P, et al. Dynamic modelling of CO_2 absorption for post
446 combustion capture in coal-fired power plants. Fuel, 2009, 88(12): 2455-2462.
447 [12]. Lawal A, Wang M, Stephenson P, et al. Demonstrating full-scale post-combustion CO_2 capture
448 for coal-fired power plants through dynamic modelling and simulation. Fuel, 2012, 101: 115-128.
449 [13]. Liu X, Chen J, Luo X, et al. Study on heat integration of supercritical coal-fired power plant with
450 post-combustion CO_2 capture process through process simulation. Fuel, 2015, 158: 625-633.
451 [14]. Canepa R, Wang M, Biliyok C, et al. Thermodynamic analysis of combined cycle gas turbine
452 power plant with post-combustion CO_2 capture and exhaust gas recirculation. Proceedings of the
453 Institution of Mechanical Engineers, Part E: Journal of Process Mechanical Engineering, 2013,
454 227(2): 89-105.
455 [15]. Luo X, Wang M. Study of solvent-based carbon capture for cargo ships through process
456 modelling and simulation. Applied Energy, 2017, 195: 402-413.
457 [16]. Fernandes J L, Verstraete J J, Pinheiro C I C, et al. Dynamic modelling of an industrial R2R FCC
458 unit. Chemical engineering science, 2007, 62(4): 1184-1198.
459 [17]. Pashikanti K, Liu Y A. Predictive modeling of large-scale integrated refinery reaction and
460 fractionation systems from plant data. Part 2: Fluid catalytic cracking (FCC) process. Energy &
461 Fuels, 2011, 25(11): 5298-5319.
462 [18]. Johansson D, Franck P A, Berntsson T. CO_2 capture in oil refineries: assessment of the capture
463 avoidance costs associated with different heat supply options in a future energy market. Energy
464 conversion and management, 2013, 66: 127-142.
465 [19]. dos Santos L T, Santos F M, Silva R S, et al. Mechanistic insights of CO_2-coke reaction during
466 the regeneration step of the fluid cracking catalyst. Applied Catalysis A: General, 2008, 336(1):

467 40-47
468 [20]. Takatsuka T, Sato S, Morimoto Y, et al. A reaction model for fluidized-bed catalytic cracking of
469 residual oil. Int. Chem. Eng, 1987, 27(1): 107-116.
470 [21]. Gupta R K, Kumar V, Srivastava V K. A new generic approach for the modeling of fluid catalytic
471 cracking (FCC) riser reactor. Chemical engineering science, 2007, 62(17): 4510-4528.
472 [22]. Oliveira L L, Biscaia E. Catalytic cracking kinetic models. Parameter estimation and model
473 evaluation. Industrial & engineering chemistry research, 1989, 28(3): 264-271.
474 [23]. Van Landeghem F, Nevicato D, Pitault I, et al. Fluid catalytic cracking: modelling of an industrial
475 riser. Applied Catalysis A: General, 1996, 138(2): 381-405.
476 [24]. AspenTech. Aspen RefSYS Option Guide; AspenTech: Cambridge, MA, 2006.
477 [25]. AspenTech. Aspen Plus FCC User's Guide Option Guide; AspenTech: Cambridge, MA, 2006.
478 [26]. Fernandes J L, Pinheiro C I C, Oliveira N M C, et al. Steady state multiplicity in an UOP FCC
479 unit with high-efficiency regenerator. Chemical Engineering Science, 2007, 62(22): 6308-6322.
480 [27]. Johansson D, Rootzén J, Berntsson T, et al. Assessment of strategies for CO_2 abatement in the
481 European petroleum refining industry. Energy, 2012, 42(1): 375-386.
482 [28]. Al-Riyami, Badr Abdullah, Jiri Klemeš, and Simon Perry. Heat integration retrofit analysis of a
483 heat exchanger network of a fluid catalytic cracking plant. Applied Thermal Engineering, 2001,
484 21(13): 1449-1487.
485 [29]. Mello LF, Gobo R, Moure GT, Miracca I. Oxy-Combustion Technology Development for Fluid
486 Catalytic Crackers (FCC) – Large Pilot Scale Demonstration. Energy Procedia 2013; 37:7815-
487 7824.
488 [30]. de Mello L F, Pimenta R D M, Moure G T, et al. A technical and economical evaluation of CO_2

capture from FCC units. Energy Procedia, 2009, 1(1): 117-124.

[31]. Hsu, Chang Samuel, and Paul Robinson, eds. Practical advances in petroleum processing. Vol. 1. Springer Science & Business Media, 2007.

[32]. Dugas ER. Pilot plant study of carbon dioxide capture by aqueous monoethanolamine. M.S.E. Thsis, University of Texas, Austin, USA, 2006.

[33]. Aboudheir A, Tontiwachwuthikul P, Chakma A, et al. Kinetics of the reactive absorption of carbon dioxide in high CO_2-loaded, concentrated aqueous monoethanolamine solutions. Chemical Engineering Science, 2003, 58(23): 5195-5210.

[34]. Aspen Plus® Rate Based model of the CO_2 capture process by MEA using Aspen Plus®. Aspen Technology Inc, Cambridge, MA, USA, 2008.

[35]. Sinnot RK. Chemical engineering design. Vol 6, 4th Ed. Oxford: Elsevier Butterworth-Heinemann, 2005.

[36]. Shah R K, Sekulic D P. Fundamentals of heat exchanger design. John Wiley & Sons, 2003.